

Combined effect of magnetic field and hydrostatic pressure on the transitions exhibited by Ni-Mn-In metamagnetic shape memory alloy

P. Lázpita^{1,2}, V. A. L'vov^{3,4}, J. Rodríguez Fernández⁵, J.M. Barandiaran², V.A. Chernenko^{1,2,6}

¹Basque Center for Materials, Applications and Nanostructures, BCMaterials, Leioa 48940, Spain

²University of the Basque Country, UPV/EHU, Leioa 48940, Spain

³Taras Shevchenko National University, Kyiv 01601, Ukraine

⁴Institute of Magnetism NASU and MESU, Kyiv 03142, Ukraine

⁵CITIMAC, Facultad de Ciencias, University of Cantabria, Santander 39005, Spain

⁶Ikerbasque, Basque Foundation for Science, Bilbao 48013, Spain

Abstract

We present a systematic study of the martensitic and magnetic transitions in the prototype metamagnetic shape memory alloy $\text{Ni}_{50}\text{Mn}_{34.5}\text{In}_{15.5}$ under hydrostatic pressure and combined pressure and magnetic field. Pressure extends the area of stability of the antiferromagnetic martensitic phase. At low magnetic field the pressure variations of the Curie temperatures of austenite, T_{CA} , and martensite, T_{CM} , show opposite signs. This is described as arising from a weak long-range antiferromagnetic state of martensite in the framework of the Landau thermodynamic model, allowing to calculate the volume magnetoelastic constants. A correlation between the signs of the pressure shifts of T_{CA} , and T_{CM} and the distance between Mn-Mn nearest neighbours is established, which matches the empirical Castelliz-Kanomata diagram. The martensitic transformation (MT) entropy, ΔS_{MT} , grows up when the MT temperature, T_M , is approaching T_{CA} under the influence of pressure, but under constant pressure this dependence is inverse. The estimated entropy change, $\Delta S_H(T)$, under magnetic field shows only a tiny increment of the inverse magnetocaloric effect under pressure, in line with recent thermodynamic and *ab initio* calculations.

1. Introduction

Magnetic solid-state refrigeration based on the magnetocaloric effect (MCE) has been proposed as a low cost, eco-friendly and energy-efficient technology for the everyday

applications displaying several advantages over the conventional gas-compression one. The compounds, such as Gd-Si-Ge [1], La-Fe-Si-H [2] or Mn-Fe-P(As,Ge) [3], exhibit giant MCE due to the first-order magnetostructural phase transformation (MSPT), which allows to heat them up, when the magnetic field, H , is applied, or to cool down, when the field is removed. Recently, the Heusler-type Ni-Mn-(In,Sn,Sb) metamagnetic shape memory alloys (MetaMSMAs), exhibiting MSPT of the martensitic type, have been also proposed as promising candidates for the magnetic solid-state refrigeration (see Ref. [4] and references therein). MetaMSMA entails a huge drop of its magnetisation, $M(T, H)$, in the temperature range of MSPT from the high-temperature ferromagnetic austenite (FMA) to the low-temperature weakly magnetic martensite. An inverse MCE, that consists in cooling down when the magnetic field is applied and heating up when it is removed adiabatically, is associated to such type of martensitic transformation. Large changes of magnetization, ΔM , and isothermal entropy, ΔS_H , are induced in this temperature range by the application of a magnetic field. The large entropy change is the precondition to obtain high values of the magnetic field induced adiabatic temperature change, $\Delta T(H, T)$.

It has been shown in many works that the entropy change in the interval of MSPT in MetaMSMAs can be effectively modified by tuning the composition, doping with magnetic (Fe, Co) and/or nonmagnetic (Cu, Al, Ti, W etc.) elements, as well as by heat treatment [5–10]. These procedures result in the changes of the electron density states and volume of the unit cell, which control the structural and magnetic stabilities, as well as the magnetic interactions in the alloys. All these changes are important for the achievement of a large $\Delta S(H)$ [11].

From a technological point of view, large values of $\Delta T(H, T)$ in a wide working temperature range are essential for the magnetic refrigeration. A wide working temperature range of refrigerator can be achieved in the case of a broad peak on the temperature dependence of $\Delta S(H)$. The wide entropy peak can be peculiar to the case of successive phase transformations, if the magnetization changes, accompanying these transformations, are of the same sign and the entropy peaks corresponding to these transformations merge [12–16]. It should be noted, however, that in the case of MetaMSMAs, which show inverse MCE, the magnetic field induced entropy changes at MSPT and Curie temperatures are of opposite sign, and, therefore, a wide working temperature range is hardly expected (for more details see Ref. [4] and references therein).

Generally, the entropy of solids changes under the hydrostatic pressure, P , giving rise to the so-called barocaloric effect (BCE) [17]. For some MetaMSMAs the temperature changes under magnetic field and pressure are comparable [17], so both are effective parameters for solid-state refrigeration [18]. The multicaloric phenomenon, a superposition of MCE and BCE, is promising for applications because it enlarges the entropy change, $\Delta S(H,P)$, and expands the working temperature range. Recently, the multicaloric phenomenon was proposed as a favourable situation for observation of a large values of $\Delta T(H,P)$ under combined external stimuli [19]. In the case of Heusler-type MCE compounds, only a few experiments have been carried out (see, e.g., [20,21]), showing that the adiabatic temperature change of the combined MCE+BCE effects is larger than the sum of the individual effects: the sum of the temperature changes induced by a magnetic field of 1 T or by 250 MPa pressure was approximately equal to the superposition of a 75% lower magnetic field and 30 % lower pressure [20].

The noticeable thermal hysteresis, peculiar to MSPT in MetaMSMAs, and the high values of the required magnetic field impose essential limitations for applications of the inverse MCE [22]. Only partial and irreversible transformations are observed in moderate magnetic fields entailing a drastic reduction of MCE, especially, in the cyclic regime used for refrigeration [22,23]. A reduction of the hysteresis can significantly improve the efficiency of MCE [24]. A purposeful modification of the microstructure and chemical composition of MetaMSMAs can somewhat reduce the hysteresis of MSPT [25], but the hysteresis effect can be substantially reduced by using the magnetic field and external pressure in such a way that the material is first magnetized without pressure and then demagnetized under pressure [26].

In the present work, the combined influence of the magnetic field and hydrostatic pressure is systematically studied, experimentally and theoretically, on the prototype $\text{Ni}_{50}\text{Mn}_{34.5}\text{In}_{15.5}$ MetaMSMA, exhibiting a first-order antiferromagnetic MSPT and second-order ferromagnetic and ferrimagnetic transitions. The latter ones occur at the Curie temperatures of austenite and martensite, above and below MSPT, respectively. The characteristic temperatures of all transitions are plotted as a function of the external magnetic field and pressure, resulting in quasi-equilibrium 3D phase diagrams. A Landau-type approach is developed to describe the experimental results and to yield the values of magnetovolume constants. The weak magnetic martensitic phase is described in terms of a long-range ordered antiferromagnetic state. The influence of the pressure on the transformation entropy and the magnetic field induced entropy change is analysed.

2. Experimental

$\text{Ni}_{50}\text{Mn}_{34.5}\text{In}_{15.5}$ (at.%) MetaMSMA was fabricated by arc melting. The ingot was annealed in vacuum at 1170 K for 24 hours and subsequently water quenched. The alloy composition was confirmed by EDX analysis within an uncertainty of about 1 at.%. According to the characteristic temperatures of the martensitic transformation, the alloy is very close to the one studied in Ref. [27]. A piece of alloy was cut from the ingot, heat treated at 1170K for 20 minutes and then slow cooled to ensure a complete $L2_1$ -ordered structure. Neutron diffraction experiments were carried out at the ILL D2B instrument. The analysis shows a $L2_1$ cubic structure ($a = 6.05 \text{ \AA}$) for the austenite, and a slightly distorted 10M orthorhombic phase ($a = 4.30 \text{ \AA}$, $b = 4.62 \text{ \AA}$, $c = 5.56 \text{ \AA}$) for the martensite. Details of the structure determination and the basic characterization by means of Differential Scanning Calorimetry can be found in [27] and in the Supplementary Material of the present article.

The influence of pressure on the different transitions was studied by low-field (5mT) thermomagnetic measurements carried out with a Quantum Design MPMS (SQUID) magnetometer equipped with a high pressure chamber cell. A Zero Field Cooling - Field Cooling - Field Heating (ZFC-FC-FH) protocol was applied: first, the alloy was cooled down to 5 K at 0 T, then the magnetic field was applied and the thermomagnetization curve, $M(T)$, was measured during heating (ZFC curve) up to 320 K, followed by the measurement during cooling down to 5 K (FC curve) and the final heating up (FH curve) under the same applied magnetic field to complete the cycle. Thermomagnetization curves were recorded under different constant magnetic fields up to 5 T at different values of the hydrostatic pressures. Magnetisation loops under different constant pressure values were measured at 5 K in magnetic fields up to 5 T. A miniature piston-cylinder CuBe pressure cell (MCell-10) was used in all cases to achieve pressures from 0 to 0.96 GPa. The pressure transmitting liquid was a mixture of mineral oils. The applied pressure was measured from the superconducting transition temperature of a tiny Sn sample placed inside the cell, with an estimated error of 0.02 GPa.

3. Experimental results

3.1. Influence of pressure on the structural and magnetic transitions characteristics

Figure 1 shows the influence of pressure on the temperature dependence of the low-field magnetisation of $\text{Ni}_{50}\text{Mn}_{34.5}\text{In}_{15.5}$ (at.%) alloy. Under no pressure, $M(T)$ shows the following sequence of phase transitions on cooling: (i) ferromagnetic ordering from the paramagnetic

austenite, PMA, to a FMA phase at the Curie temperature, $T_{CA} \approx 310$ K; (ii) in the temperature range $240 \text{ K} < T < 260 \text{ K}$ the alloy transforms from FMA to the orthorhombic weak magnetic martensite, which can be tentatively considered as a weak antiferromagnetically ordered phase, AFMM, formed as a result of competing ferro – antiferro magnetic interactions (see Refs.[28–30]). The FMA→AFMM phase transformation is characterised by the abrupt decrease of the magnetisation, practically to zero. The FMA→AFMM transformation was described in Ref. [31] as a magnetically driven martensitic transformation, which can be termed as MSPT of the martensitic type. During further field cooling AFMM transforms into a ferrimagnetic martensite (FiMM), $T_{CM} \approx 223$ K, with a lower magnetisation value than the FMA. The ZFC curve exhibits a maximum, that may be attributed to the blocking temperature, below which a relaxation of the magnetization due to a frustration becomes slow compared to the time scale of measurements [32].

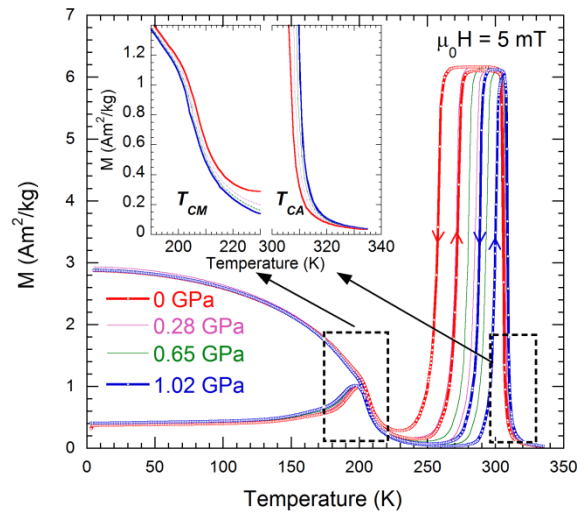


Fig. 1. ZFC – FC – FH magnetisation curves recorded at low-field (5 mT) for the different constant pressures. Inset depicts the rescaled fragments of the curves to demonstrate the opposite pressure induced shifts of Curie temperatures of martensite, T_{CM} , and austenite, T_{CA} .

Figure 1 and Inset show that the hydrostatic pressure noticeably rises the MSPT temperature, T_M , elevates the Curie temperature of the austenite, T_{CA} , and lowers the temperature of the AFMM ↔ FiMM transition, T_{CM} . As a result, high pressure drastically narrows the temperature interval of stability of the FMA phase, whereby stabilises the AFMM phase. The characteristic temperatures of the transitions were determined by the maximum of the first derivative of $M(T)$ for the forward MSPT, T_M , and by the two-tangents method for the two magnetic transitions. The resulting numerical values are plotted in Fig. 3 as a function of pressure, giving rise to the $P - T$ phase diagram limiting the areas of

existence of the four mentioned phases. The influence of the small magnetic field, of 5 mT, on this diagram can be neglected.

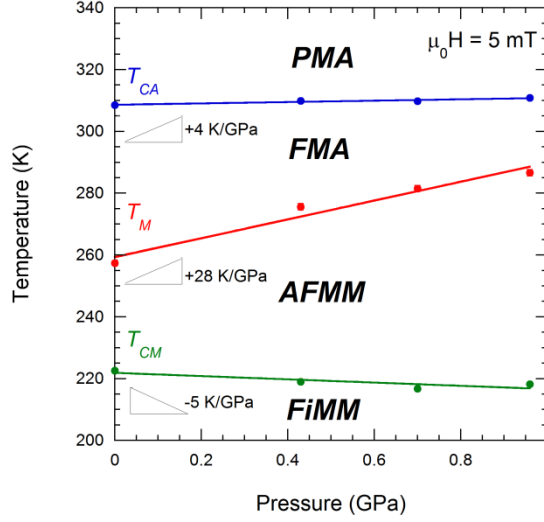


Fig. 2. Experimental $T - P$ diagram of the phase transitions exhibited by $\text{Ni}_{50}\text{Mn}_{34.5}\text{In}_{15.5}$ (at.%) alloy. It is approximated by straight lines limiting the areas of existence of the paramagnetic austenite (PMA), ferromagnetic austenite (FMA), antiferromagnetic martensite (AFMM) and ferrimagnetic martensite (FiMM). The values of the slopes are indicated.

The values of the slopes are shown in Fig. 2 and listed below:

$$\begin{aligned} dT_M / dP &\approx 28 \text{ K/GPa}, \\ dT_{CA} / dP &\approx 4 \text{ K/GPa}, \\ dT_{CM} / dP &\approx -5 \text{ K/GPa}. \end{aligned} \quad (1)$$

It is worth noting that the value of dT_M/dP in Eq. (1) lies in the wide range of (18 – 60) K/GPa reported in the literature for different Heusler type MetaMSMAs [33–38]. The literature provides also quite a wide spread of the experimental values of dT_{CA}/dP for these alloys, ranging between zero [33] and 6 K/GPa [36]. Such a broad variation is, obviously, the result of their strong dependence on the composition and degree of atomic order (see e.g. Ref. [39,40]). Incidentally, the value of dT_{CM}/dP has never been measured before. The reliable negative value of this parameter shown in Eq.(1) is a significant finding of the present work. The numerical values of the pressure induced shifts of the characteristic temperatures, listed in Eq.(1), represent crucial inputs for developing any theoretical approach, as that described in the next sections.

3.2. Combined effect of high-field and pressure on magnetostructural phase transformation

Figure 3 shows the magnetisation during heating for three values of magnetic field in zero pressure and under a pressure of 0.96 GPa. One can conclude that the main influence of pressure is the shift of MT, while its influence on the magnetisation of the FMA phase is small, as the solid and dashed lines almost coincide in the temperature range of stability of the FMA. Due to this, the decrease of the magnetisation under pressure (see Inset in Fig. 3) is proportional to the shift of the MSPT temperature, $T_M(P) - T_M(0)$.

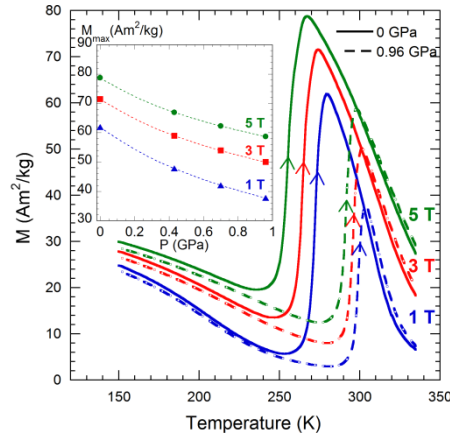


Fig. 3. Combined effect of a strong magnetic field and pressure on the temperature dependence of magnetisation. Only selected heating curves at 0 and 0.96 GPa are shown for the clarity. Inset demonstrates the pressure dependences of the maximums on the $M(T)$ curves at different values of magnetic field.

From the thermomagnetisation data, in the absence of pressure, the transformation temperature shift can be estimated as:

$$dT_M / d(\mu_0 H) \approx -5 \text{ K/T}. \quad (2)$$

This is also an important parameter for the subsequent theoretical treatment.

Using the experimental data of Fig. 3, a 3D T - P - H phase diagram of the magnetostructural transformation is now plotted in Fig. 4(a). The diagram illustrates the simultaneous influence of the magnetic field and hydrostatic pressure on the MT temperature and can be used to predict the values of T_M at any combination of P and H in the studied ranges and beyond. The projections of the $T_M(H, P)$ surface on the $T_M - H$ and $T_M - P$ planes are reproduced in Fig. 4 (b) for better visibility.

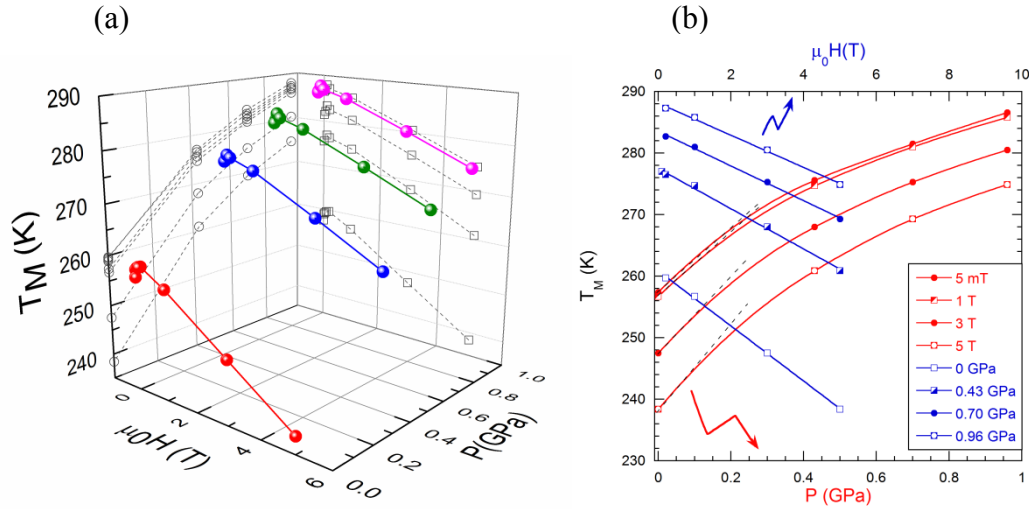


Fig 4. A combined influence of the magnetic field and hydrostatic pressure on the temperature of magnetostructural phase transformation in $\text{Ni}_{50}\text{Mn}_{34.5}\text{In}_{15.5}$ (at.%) alloy: (a) 3D T - P - H phase diagram; (b) T_M dependencies projected onto the T - P and T - H planes.

Figure 4 (b) shows a linear decrease of the MT temperature as a function of magnetic field at different constant values of pressure. As it is seen, an increasing of pressure leads to the reduction of the field induced transformation temperature shift dT_M/dH . Note, that the value given by Eq. (2), is obtained in the absence of hydrostatic pressure.

The MT temperature of the alloy increases under compression, which is opposite to the T_M versus H behaviour. Fig. 4(b) illustrates an interesting result: T_M remains practically unchanged under the combined influence of $\mu_0H \sim 5\text{ T}$ and $P \sim 0.5\text{ GPa}$. The dependence of T_M on pressure is nonlinear, but for the sake of convenience, the value for dT_M/dP , shown in Eq.(2), corresponds to the linear interpolation of the T_M values obtained at $\mu_0H = 5\text{ mT}$ for $P = 0$ and $P = 0.96\text{ GPa}$.

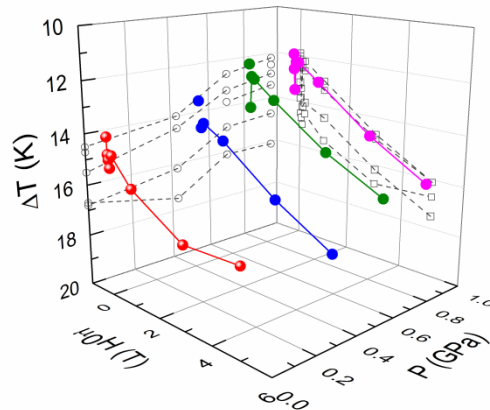


Fig. 5. Combined influence of the magnetic field and hydrostatic pressure on the hysteresis, ΔT , of the magnetostructural phase transformation. Note the reverse orientation of the Y-axis for better clarity.

The 3D diagram in Fig. 5 displays the combined influence of the magnetic field and hydrostatic pressure on the thermal hysteresis of magnetostructural phase transformation, ΔT , determined as the difference between the temperatures of the reverse (martensite-austenite) and forward (austenite-martensite) transformation temperatures. Fig. 5 shows that ΔT is a decreasing function of pressure and increasing function of magnetic field. The decrement of the hysteresis under pressure is about of -3 K/GPa; and its increment under magnetic field is close to 0.6 K/T. The increase of ΔT as a function of magnetic field is related to the thermodynamic and/or kinetic “arrest” of the transformation, an empirically well-known phenomenon in MetaMSMA [41]. Naturally, the application of the pressure tends to remove the influence of field, whereby decreasing the value of hysteresis.

4. Influence of pressure on transformation entropy change

The experimental magnetisation curves in Fig. 3 allow to obtain not only the values of the derivative dT_M / dH (Eq. (2)), but also the jump-like change of magnetization, ΔM , at T_M . These data provided an input to the Clausius-Clapeyron relation, adapted here for the magnetic case, and used to investigate the entropy change at MT:

$$\Delta S(H, P) = - \left[\frac{dT_M(P)}{dH} \right]^{-1} \Delta M(H, P) \quad (3),$$

Fig. 6 shows the calculated results of $\Delta S(H, P)$ plotted as a function of the distance between T_{CA} and T_M , the two characteristic temperatures being dependent on the magnetic field and pressure. The difference $(T_{CA} - T_M)$ has been used in many reports as a generalized “order parameter” to characterize the “structure – magnetism” correlation (see, e.g., [42] and references therein).

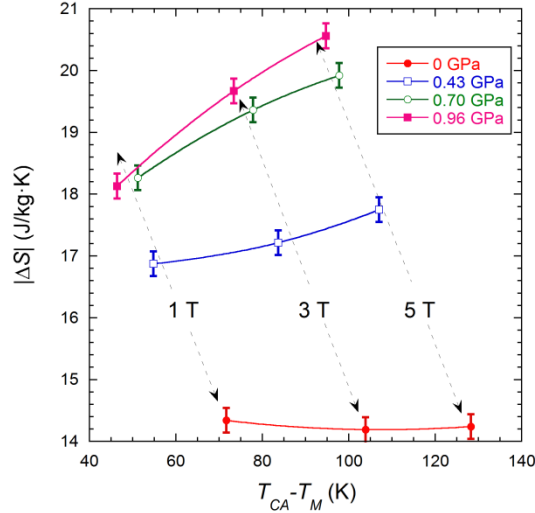


Fig. 6. Entropy change at the martensitic transformation, calculated from Eq.(3), as a function of the generalized “order parameter” ($T_{CA} - T_M$). The dependencies are strongly affected by the combined influence of pressure and magnetic field. Lines are guides to the eyes. Dashed lines show the points measured at the indicated values of the magnetic field.

For $P = 0$, ΔS presents a monotonous decrease with the "order parameter" ($T_{CA} - T_M$), which is almost the same as the one obtained in Ref. [42]. Fig. 6 shows that the pressure overturns the decreasing tendency commonly observed at $P=0$ in Refs. [42,43]. At the highest pressure (0.96 GPa) the simultaneous small increment of ΔM and the considerable decrement of the dT_M/dH result in a large increase of ΔS , reaching a value of $-20 \text{ J/K}\cdot\text{kg}$ at 5 T (30% higher than at $P=0$).

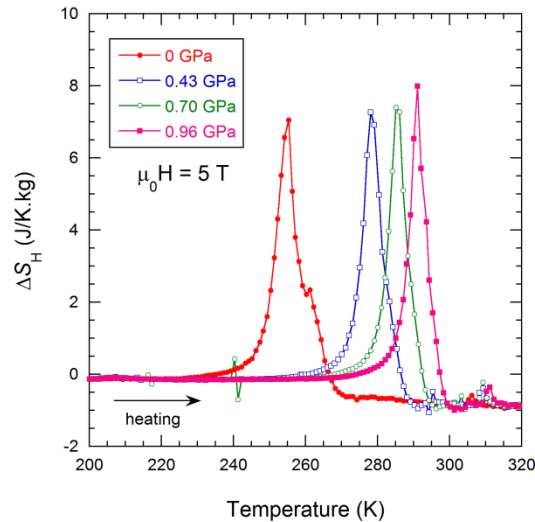


Fig. 7. Illustration of the inverse magnetocaloric effect in $\text{Ni}_{50}\text{Mn}_{34.5}\text{In}_{15.5}$ at $\mu_0H=5\text{T}$ at different constant pressures. The magnetic field-induced entropy change, ΔS_H , was calculated by Maxwell relationship using the data in Fig. 3, i.e. on heating. Cooling curves give similar results.

It is now instructive to estimate the influence of hydrostatic pressure on the magnetic field induced entropy change, ΔS_H , near MSPT and compare with the data for ΔS depicted in Fig. 6. Recently, it was shown that the application of the Maxwell relationship for an approximate evaluation of the inverse magnetocaloric effect in the vicinity of first-order MSPT is possible if the spontaneous magnetization of material is included [4]. Accordingly, the results from Fig. 3 have been used to calculate the temperature evolution of the magnetic field induced entropy change, $\Delta S_H(T)$, by the standard expression:

$$\Delta S_H(T) = \int_{H_1}^{H_2} \frac{\partial M(T, H)}{\partial T} dH \quad (4)$$

Figure 7 shows the evolution of $\Delta S_H(T)$ under different pressures. One can see that, pressure increases the maximum of the $\Delta S_H(T)$ curves only slightly, and the maximum values of ΔS_H are much lower than ΔS values estimated by the Clausius-Clapeyron equation. This is not surprising as Clausius-Clapeyron assumes a sudden change of the magnitudes, like magnetization or entropy, at the transformation, while Maxwell equation applies to energy functions that are continuous and with continuous derivatives, up to the second order at least, in all the studied range. On the other hand, it is very reasonable to assume that there exists some correlation between calculated value of ΔS (or determined by DSC) and the calculated $\Delta S_H(T)$, but both experiments and theory do not confirm that this correlation is direct. Recent thermodynamic [4,44] and ab initio analyses [45] have shown that magnetization anomalies (no matter which mechanism is behind the large changes on $M(T)$ at different magnetic fields) are the main ingredients which determine the MCE response

5. Effect of pressure on the magnetic exchange coupling

Our precise measurements enabled to detect opposite pressure shifts of the Curie temperatures of austenite, T_{CA} , and martensite, T_{CM} (Fig. 2). This behaviour is found for the first time and deserves a more detailed discussion.

The effect of pressure on the exchange interaction integral, J , and the corresponding behaviour of T_C , was studied for Ni_2MnSn -based compounds using density functional theory (DFT) [46]. Two different tendencies of J were disclosed depending on the Mn-Mn interatomic distances. At large Mn-Mn distances, pressure shortening of the Mn-Mn bonds leads to a reduction of the exchange interaction and to the decrease of T_C . This is due to the band broadening which increases the overlap of the electronic states, and therefore reduces the local magnetic moment. The opposite tendency of T_C , observed for large Mn-Mn

distances, is explained as the result of the increment of the electron hopping which yields a stronger spin exchange interaction between the magnetic atoms. A competition between these two opposite trends can explain the behaviour observed in the present work.

It is well established that in off-stoichiometric Ni-Mn-In compounds, Mn atoms occupy preferably two different sublattices (Mn and In ones) entailing two different Mn-Mn interatomic distances. Consequently, there are two different exchange constants: $J_{\text{Mn-Mn}}$ between the Mn atoms sited at the Mn sublattices (Mn1) (large distances), and $J'_{\text{Mn-Mn}}$ between Mn atoms at the Mn sublattice and the Mn at the In (Mn2) one (short distances). Considering that in the austenitic phase $J_{\text{Mn-Mn}}$ is much stronger than $J'_{\text{Mn-Mn}}$, a positive variation of T_{CA} under applied pressure should be observed. The situation is the opposite in the martensitic phase, where the magnetic coupling is controlled by $J'_{\text{Mn-Mn}}$ between nearest neighbours, which is typically antiferromagnetic. In this case, the pressure induces a decrease of T_{CM} .

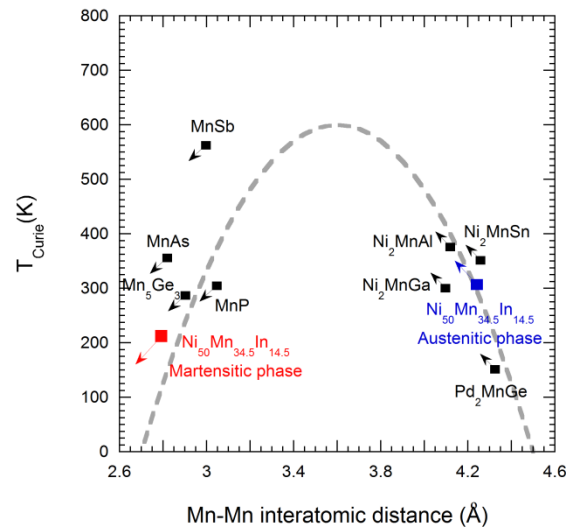


Fig.8. The Castelliz-Kanomata empirical dependence of the exchange interaction showing the Curie temperature as a function of the interatomic Mn-Mn distance in various Mn-based compounds, such as pnictides and Heusler alloys [40,46,47]. The studied in the present work Heusler-type MetaMSMA is represented by blue in the austenitic state and by red in the martensitic one. Arrows up and down stand for positive and negative values of the derivative dT_C/dP , respectively.

Note, that such an opposite behaviour of T_C in austenite and martensite is in line with the Castelliz-Kanomata empirical curve, shown in Fig. 8 [40,46,47]. This curve displays the dependence of T_C as a function of the nearest interatomic distance between the manganese atoms in different manganese-based compounds, whereby one can predict the sign of the pressure-induced T_C shift as indicated in Fig. 8. At large distances (≈ 4.50 Å), $dT_C/dP > 0$ but

it decreases to a minimum value (close to zero) at about 3.6 Å. Below this distance the pressure induces the contrary effect, i.e., $dT_C/dP < 0$, increasing its absolute value down to the shortest distance (2.80 Å). In the studied compound, the Mn-Mn distances in the austenite, determined from the L_{21} cubic unit cell parameter, are $d_{\text{Mn1-Mn1}}^A = 4.24$ Å and $d_{\text{Mn1-Mn2}}^A = 3.02$ Å. So, the experimentally measured $dT_C/dP > 0$ indicates that T_{CA} is determined essentially by the Mn atoms sited at their main positions, whereas the effect of Mn placed at the In positions is negligible. In the martensitic phase, represented by the 10M orthorhombic unit cell, the distance between the nearest Mn atoms is $d_{\text{Mn1-Mn2}}^M = 2.78$ Å and the largest one is $d_{\text{Mn1-Mn1}}^M = 4.62$ Å. The measured negative evolution of T_{CM} with the pressure, points out that the Mn nearest-neighbours do determine the behaviour of T_{CM} . So, in Ni-Mn-In a 10 % of the reduction in the Mn-Mn interatomic distances occurs during cooling MT, which produces a volume drop, as well as a change in the sign of the exchange constant, from ferro- to antiferromagnetic, typical for many magnetic compounds and rare earth elements (see [40,47] and reference there in).

Figure 9 shows the isothermal magnetization curves recorded at 5 K for several pressures.

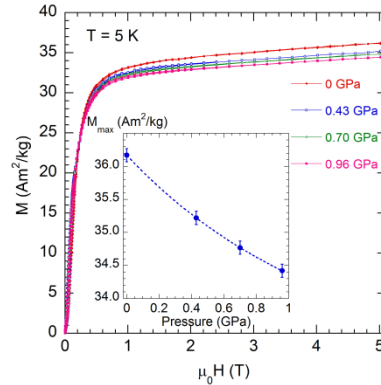


Fig. 9. Magnetization curves at constant temperature of 5 K (martensitic phase) and different pressures. Inset: pressure dependence of the maximum values of magnetization obtained at 5 T.

At all pressures, the $M(H)$ curves are not fully saturated, even at the field of 5 T, revealing an antiferromagnetic contribution in the martensitic phase. The values of the magnetization at 5 T, equal to $36.2 \text{ Am}^2\text{kg}^{-1}$ for $P=0$, present a decrease as a function of the applied pressure with a slope $d \ln M_{\text{max}}/dP = -43 \cdot 10^{-3} \text{ GPa}^{-1}$ between 0.43 and 0.96 GPa. A similar slope has been reported in other NiMn-based Heusler compounds [36]. A considerable decrement of the $M_{\text{max}}(P)$ dependence can be explained within a model of the uncompensated local moment disorder proposed for Kamarad et al. [48] for NiMn-based MetaMSMAs. This model illustrates a high sensitivity of the total magnetization to the atomic order and the

external pressure. Both two control the Mn-Mn interatomic distances, leading to the tendency of the magnetic coupling inversion from ferromagnetic to antiferromagnetic. Particularly, values of the parameter $d\ln M_{\max}/dP$, equal to $-8 \cdot 10^{-3} \text{ GPa}^{-1}$ and $-38 \cdot 10^{-3} \text{ GPa}^{-1}$, have been determined for the ordered and disordered Ni_3Mn alloys, respectively, showing a high impact of the atomic disorder on this parameter [48]. The enhanced value of $d\ln M_{\max}/dP$ obtained in this work is indicative of a certain degree of disorder related to the high Mn content and, as a result, the presence of antiferromagnetic coupling due to the reduction of the Mn-Mn distances. This behaviour is also compatible with the huge difference between the experimental magnetic moment of $1.7 \mu_{\text{B}}/\text{f.u.}$ (5K and 0 GPa), and the theoretical one of $2.4 \mu_{\text{B}}/\text{f.u.}$ The latter value was calculated by assuming that the magnetic moments for Ni and Mn atoms are $0.2 \mu_{\text{B}}$ and $3.2 \mu_{\text{B}}$, respectively, and that all Mn atoms located on the In sublattice are coupled antiferromagnetically with all Mn atoms placed on their proper sites. The mismatch between values of magnetic moments infers that there is some degree of disorder, which reduces the total magnetic moment. According to the calculated values, not only Mn atoms sited at In places, but also a 7% more of the total Mn atoms, are coupled AFM. This indicates that there is a partial disorder in which Mn atoms could occupy also the Ni sublattice. Nevertheless, part of the magnetic moment reduction can also be related to the local spin canting induced by the atomic modulation in the martensitic phase [49,50] or to a high density of antiphase boundaries associated to the presence of dislocations in the bulk, which results in an increment of the shortest distance Mn-Mn neighbours that couple antiparallel to the ferromagnetic matrix [51].

6. Theoretical treatment

6.1. Influence of pressure on the Curie temperatures of austenite and martensite, evaluation of magnetoelastic constants

The especially important finding of the present work that the shifts of T_{CA} and T_{CM} under pressure appeared to be of the opposite signs was already explained in Sec. 5. According to the empirical Castellitz-Kanomata rule, the sign of the pressure-induced shift of the Curie temperature in different compounds is determined by the distance between the manganese atoms: the shift is positive if the distance is larger than 0.36 nm and negative below this value. Whereas the positive value of dT_{CA}/dP , Eq. (1), is very typical for Heusler-type MSMA (see Sec.3.1), a negative pressure shift of T_C , already well known for Invar-type

alloys, is found in this work for T_{CM} . Therefore, a special theoretical analysis is needed to substantiate the possibility of negative pressure shift of T_{CM} and its implications.

It was already mentioned that a first-principles study of the pressure influence on the Curie temperature in the stoichiometric Ni₂MnSn Heusler compound was carried out in Ref. [46]. It demonstrated that the Mn-Mn exchange interaction within the first and fourth coordination spheres can change sign when the applied pressure diminishes the Mn-Mn distance to 0.34 nm, but the pressure required is quite high. On the other hand, disorder and defects, giving rise to atomic interchanges between Ni and Mn sublattices [48] increase the influence of pressure on the magnetic properties of Ni-Mn-Sn alloy [36], as suggested by the dependence of the magnetic properties of MetaMSMAs on the thermal treatments [40]. It should be also stressed, that ZFC and FC magnetisation curves are entirely different in the temperature interval of FMM state (see Fig. 1) hinting for a strong dependence of the magnetic properties of the alloy on the micro- and nanostructure of the martensite. Besides, ferromagnetic resonance, FMR, in twinned martensitic films of Ni-Mn-Sn-Co points to the antiferromagnetic coupling between the twins [30]. Finally, the transformation properties of Ni-Mn-In [31] and magnetocaloric effect in Ni-Mn-Sn [4,44] were satisfactorily described using a macroscopic model of magnetic solid with two magnetic sublattices: \mathbf{M}_1 and \mathbf{M}_2 .

The model is based on the following equations for the Gibbs potential, G :

$$\begin{aligned}
 G &= G_m + G_{me}, \\
 G_m &= J_0(\mathbf{M}_1^2 + \mathbf{M}_2^2) + J_{12}\mathbf{M}_1\mathbf{M}_2 - (\mathbf{M}_1 + \mathbf{M}_2)\mathbf{H}, \\
 G_{me} &= -\delta_1(\mathbf{M}_1^2 + \mathbf{M}_2^2)v - 2\delta_{12}\mathbf{M}_1\mathbf{M}_2v,
 \end{aligned} \tag{4}$$

where G_m is the sum of exchange and Zeeman energy, J_0 and J_{12} are temperature-dependent exchange parameters. G_{me} is the magnetoelastic energy, which describes the dependence of the exchange energy on the specific volume of the MetaMSMA, δ_1 and δ_{12} are magnetoelastic constants, v is the relative volume change, which may be caused by the hydrostatic pressure, spontaneous and forced magnetostriction and/or a magnetostructural phase transformation of the martensitic type.

Using the Gibbs potential, Eq. (4), it is possible to consider the sequence of phase transformations “paramagnetic austenite - ferromagnetic austenite - antiferromagnetic martensite - ferromagnetic martensite” (PMA→FMA→AFMM→FiMM). As it is shown

below, these phase transitions provide a satisfactory theoretical model describing the experimentally observed phase transitions (Fig.2).

Mathematical expressions, similar to Eq.(4), are currently used in the theory of ferro- and antiferromagnetism (see e.g. [52]). In the case that $|\mathbf{M}_1| = |\mathbf{M}_2|$ holds, the relationship $\mathbf{M}_1 \approx -\mathbf{M}_2$ is valid for the ferromagnetic or antiferromagnetic solid in a weak magnetic field. For austenite the relative volume change under pressure is equal to $-P/B$, where B is bulk modulus; for martensite it is equal to $(-P/B) + v_{tr}$, where $v_{tr} = (V_M - V_A)/V_A$ is the relative volume change as a result of the MT. Due to this, the Gibbs potential can be expressed as

$$G = \frac{1}{2} J(T, P) M^2(T, P), \quad (5)$$

where

$$J(T, P) = \frac{1}{2} [J_0(T) + J_{12}(T)] + (\delta_1 + \delta_{12}) \frac{P}{B} \equiv J_{fm,a}(T, P), \quad (6)$$

for ferromagnetic austenite,

$$J(T, P) = \frac{1}{2} [J_0(T) - J_{12}(T)] - (\delta_1 - \delta_{12}) \left(v_{tr} - \frac{P}{B} \right) \equiv J_{afm,m}(T, P), \quad (7)$$

for antiferromagnetic martensite, and

$$J(T, P) = \frac{1}{2} [J_0(T) + J_{12}(T)] - (\delta_1 + \delta_{12}) \left(v_{tr} - \frac{P}{B} \right) \equiv J_{fm,m}(T, P), \quad (8)$$

for ferromagnetic martensite. $M = |\mathbf{M}_1 + \mathbf{M}_2|$ is the modulus of the magnetization. Taking into account that in the absence of external magnetic field the magnetization is equal to zero in the paramagnetic and antiferromagnetic phases, the pressure-induced shifts of the PMA→FMA and FMA→FMM phase transformations temperatures can be found from the equations

$$J_{fm,a}(T, P) - J_{fm,a}(T, 0) = 0, \quad (9)$$

and

$$J_{fm,m}(T, P) - J_{fm,m}(T, 0) = 0, \quad (10)$$

respectively. In accordance with the Landau theory of phase transitions, the exchange parameters involved in Eqs.(6) and (7) depend linearly on the temperature in the vicinity of the PMA→FMA and FMA→FMM transformation temperatures, that is

$$J_{fm,a}(T, P) = (\xi / M_0^2) [T - T_{CA}(P)] / T_{CA}(0), \quad (11)$$

$$J_{fm,m}(T, P) = (\xi / M_0^2)[T - T_{CM}(P)] / T_{CM}(0), \quad (12)$$

where $M_0 = |\mathbf{M}_1(0)| + |\mathbf{M}_0(0)|$ is a low-temperature limit of magnetization in the ferromagnetic phase. The material constant ξ , involved in the Eq. (11), is approximately equal to 0.1 GPA for the Heusler MSMA, which undergo the PMA→FMA transformation [53]. This constant prescribes a certain value of the derivative $dJ_{fm,a} / dT$. The same constant is used in Eq. (12), assuming that the antiferromagnetic exchange coupling, described by the parameter J_{12} , is much weaker than the ferromagnetic one, described by the parameter J_0 , and therefore, $dJ_{fm,a} / dT \approx dJ_{fm,m} / dT$. Combining Eqs. (6), (9) and (11), one can express the pressure-induced shift of the Curie temperature of the austenite as

$$\Delta T_{CA}(P) \equiv T_{CA}(P) - T_{CA}(0) \approx -(\delta_1 + \delta_{12})M_0^2 P T_{CA}(0) / \xi B, \quad (13)$$

whereas Eqs. (7), (10) and (12) result in the following expression for the Curie temperature of the martensite

$$\Delta T_{CM}(P) \equiv T_{CM}(P) - T_{CM}(0) \approx -2\delta_{12}M_0^2 P T_{CM}(0) / \xi B. \quad (14)$$

The experimental values of these parameters are: $T_{CA} \approx 310$ K, $T_{CM} \approx 225$ K, $\Delta T_{CA} \approx 4$ K, $\Delta T_{CM} \approx -5$ K for $P \approx 0.96$ GPa. Using the value $M_0 \approx 1000$ emu/cm³, which is typical of Ni-Mn-In alloys, and a bulk modulus $B \approx 150$ GPa, typical of Heusler-type MSMA, one can roughly estimate the dimensionless magnetoelastic constants $\delta_1 = -3.752 \times 10^3$, $\delta_{12} = 1.736 \times 10^3$ and the magnetoelastic constant

$$\delta_0 = \frac{3}{2}(\delta_1 + \delta_{12})M_0^2 \approx -0.3 \text{ GPa}, \quad (15)$$

which is traditionally used for description of the magnetoelastic coupling in ferromagnetic SMAs. The estimated constant, Eq. (15), is rather close to the value of -0.4 GPa reported for the Ni₂MnGa alloy [53].

The most important point is that the magnetoelastic coupling in MetaMSMA with two magnetic sublattices is described by the two magnetoelastic constants. The difference in the signs of the shifts of Curie temperatures cannot be explained using the expression for the magnetoelastic energy of a single lattice ferromagnet, which involves only one magnetoelastic constant. The opposite signs of the observed shifts of the austenite and martensite Curie temperatures under hydrostatic pressure imply that the magnetoelastic constants have also different signs.

It should be noticed that the values $|\delta_1|$ and δ_{12} , estimated above for the $\text{Ni}_{50}\text{Mn}_{34.5}\text{In}_{15.5}$ alloy, are smaller, by one order of magnitude, than those used for the description of magnetically induced MT in $\text{Ni}_{45}\text{Mn}_{36.7}\text{In}_{13.3}\text{Co}_5$ (at%) [31]. However, one should take into account that the Curie temperature is noticeably lower, and the influence of the magnetic field on magnetisation in the ferromagnetic phase is much more pronounced in $\text{Ni}_{50}\text{Mn}_{34.5}\text{In}_{15.5}$ (at.%) than in $\text{Ni}_{45}\text{Mn}_{36.7}\text{In}_{13.3}\text{Co}_5$. These differences mean that the exchange parameter $J_{fm,a}(T, 0)$ is noticeably smaller for $\text{Ni}_{50}\text{Mn}_{34.5}\text{In}_{15.5}$. Due to this, the real values of $|\delta_1|$ and δ_{12} , which characterize the dependence of the exchange parameters on the volume, may be comparatively small, as well. Therefore, the quantitative theoretical description of the transformation behaviour of Ni-Mn-In alloy, using the values of the magnetoelastic constants estimated above, needs further consideration.

6.2. Influence of pressure on the characteristic temperatures of the magnetostructural phase transformation

To begin with, let us imagine that the MT temperature, T_M , coincides with the temperature of the magnetic transition from ferromagnetic to antiferromagnetic, T_0 , and therefore, both characteristic temperatures coincide with the temperature of the magnetostructural phase transformation, MSPT.

As the exchange parameter, Eq.(7), depends on v_{tr} , assuming v_{tr} independent of pressure, one can estimate the influence of pressure on T_0 from Eqs.(6) and (7) and the equations

$$\begin{aligned} J_{afm,m} - J_{fm,m} &= -J_{12}(T) + 2\delta_{12}(v_{tr} - P/B), \\ J_{afm,m} - J_{fm,m} &= (\xi_{12}/M_0^2)[T - T_0(P)]/T_0(0). \end{aligned} \quad (16)$$

All these equations result in the approximation

$$\Delta T_0(P) \equiv T_0(P) - T_0(0) \approx 2\delta_{12}M_0^2PT_0(0)/\xi_{12}B > 0 \quad (17)$$

Equations (14) and (17) show that

- (i) $\Delta T_{CM}(P)$ and $\Delta T_0(P)$ have different signs;
- (ii) $\Delta T_{CM}(P)$ and $\Delta T_0(P)$ are close in absolute value, if $T_{CM}(0)$ is close to $T_0(0)$;
 $\Delta T_0(P) \gg \Delta T_{CM}(P)$, if $\xi_{12} \ll \xi$.

The point (i) is in agreement with the experimental data reported above. The experimental value $dT_{CM}/dP \approx -5$ K/GPa coincides with the theoretical one if $\zeta_{12} = 0.02$ GPa, that is if $\zeta_{12} \ll \zeta$. As it was noticed above, this inequality is fulfilled if the antiferromagnetic exchange interaction between the magnetic sublattices is much weaker than the ferromagnetic interaction inside each sublattice.

It should be remembered, however, that the change of elastic energy under pressure can contribute to the $\Delta T_0(P)$ value. It may be predicted, therefore, that if the temperatures $T_0(0)$ and $T_M(0)$ coincide, there is a possibility that hydrostatic pressure can "split" them. If $T_0(0)$ and $T_M(0)$ do not coincide, the difference between the MT temperature and the temperature of magnetic phase transition can noticeably depend on the pressure.

6.3. Influence of magnetic field on the temperature of magnetostructural phase transformation

The magnetic field derivative of MT temperature, Eq. (1), was determined using the $M(T, H)$ curves, which show the abrupt decrease in the temperature range of MSPT (see Fig. 3). In the model of MetaMSMA with two equivalent magnetic sublattices, this decrease of magnetisation is interpreted as the result of phase transformation from the ferromagnetic austenite to the antiferromagnetic martensite. Here, we will describe this phase transition in short, for more details see Ref. [31].

Let θ be the angle between the vectors \mathbf{M}_1 and \mathbf{M}_2 . The angles between the strong magnetic field and the vectors \mathbf{M}_1 and \mathbf{M}_2 are $\theta/2$ and $-\theta/2$, respectively. In absence of pressure the difference between Gibbs potentials of these phases is expressed according to Eq. (4) as

$$G_{fm,m} - G_{afm,m} = \frac{1}{4} J_{12}^*(T) M_0^2(T) (1 - \cos \theta) - H M_0(T) \left(1 - \cos \frac{\theta}{2} \right), \quad (18)$$

where $J_{12}^*(T) = J_{12}(T) - 2\delta_{12}v$. An angle θ satisfies the equation

$$\cos \frac{\theta}{2} = \frac{H}{J_{12}^*(T) M_0(T)}. \quad (19)$$

The angle θ is a decreasing function of magnetic field, which vanishes at the phase transition line in H - T plane. Therefore, the equation of this line is

$$J_{12}^*(T) M_0(T) = H. \quad (20)$$

Substituting $T_0(P)$ by $T_0(H)$ in Eq. (16), one can obtain the relationship

$$dT_0(H)/dH = -M_0[T_0(0)]T_0(0)/\xi_{12}. \quad (21)$$

The experimental values $T_0(0) \approx 260$ K, $M_0[T_0(0)] \approx 4.5 \times 10^5$ A/m and the value $\xi_{12} = 0.02$ GPa, estimated above from the experimental value $\Delta T_0(P)$, result in the estimation $dT_0(H)/dH \approx -5.7$ K/T, which is in a good agreement with the experimental value shown in Eq. (2).

7. Conclusions

In the present work, the transition behaviour of the prototype MetaMSMA, $\text{Ni}_{50}\text{Mn}_{34.5}\text{In}_{15.5}$ (at.%), has been systematically studied under hydrostatic pressure and under the combined influence of pressure and magnetic field. The following new results can be highlighted.

1. The three-dimensional phase diagram of the martensitic transformation and Curie temperatures of martensite and austenite as function of magnetic field and hydrostatic pressure has been determined. Particularly, it was found that pressure extends the area of stability of the antiferromagnetic martensitic phase.
2. The opposite signs of dT_{CA}/dP and dT_{CM}/dP in low magnetic fields is an important finding of this work, indicating a weak long-range antiferromagnetism of the martensitic phase. This behaviour is described in the framework of the Landau-type thermodynamic model applied to a magnetic solid with two ferromagnetic sublattices, which interact antiferromagnetically. Hydrostatic pressure data enabled to disclose the signs and calculate values of the volume magnetoelastic constants.
3. A correlation between the signs of the pressure shifts of Curie temperatures of austenite and martensite and the distance between the closest Mn – Mn neighbours, which matches the empirical Castelliz-Kanomata diagram, has been established.
4. We found that at constant magnetic field, the transformation entropy, ΔS , calculated using Clausius-Clapeyron relationship, strongly grows up when T_M is approaching T_{CA} under the influence of pressure. Such a trend was previously observed under high magnetic fields or for MetaMSMAs with different compositions. On the other hand, we see that ΔS versus $(T_{CA} - T_M)$ obeys this trend only at zero pressure, whereas this dependence is inverted under pressure and ΔS exhibits a strong increase.
5. It is interesting that, contrary to ΔS , the estimated magnetic field induced entropy change, $\Delta S_H(T)$, shows only a tiny increment of the maximum on the $\Delta S_H(T)$ curve under pressure.

Such a quantitative misfit between the pressure influence on $\Delta S_H(T)$ and ΔS means that not always one can expect close correlation in the behaviour of these entropies. This conclusion is in line with recent thermodynamic and *ab initio* theoretical findings [4,44].

Acknowledgements

The financial supports from Ministry of Science, Innovations and Universities (projects MAT2017-83631-C3-3-R and RTI2018-094683-B-C53-54) and from the Basque Government Department of Education (project IT1245-19) are greatly acknowledged.

REFERENCES

- [1] V.K. Pecharsky, K.A. Gschneidner, Jr., Giant Magnetocaloric Effect in $Gd_5Si_2Ge_2$, *Phys. Rev. Lett.* 78 (1997) 4494–4497. doi:10.1103/PhysRevLett.78.4494.
- [2] J. Lyubina, K. Nenkov, L. Schultz, O. Gutfleisch, Multiple Metamagnetic Transitions in the Magnetic Refrigerant $La(Fe,Si)_{13}H_x$, *Phys. Rev. Lett.* 101 (2008) 177203. doi:10.1103/PhysRevLett.101.177203.
- [3] O. Tegus, E. Brück, K.H.J. Buschow, F.R. de Boer, Transition-metal-based magnetic refrigerants for room-temperature applications, *Nature*. 415 (2002) 150–152. doi:10.1038/415150a.
- [4] V.A. Chernenko, V.A. L’Vov, E. Cesari, J.M. Barandiarán, Fundamentals of magnetocaloric effect in magnetic shape memory alloys, in: *Handb. Magn. Mater.*, Ed. E. Bruck, Elsevier, 2019: pp. 1–45. doi:10.1016/bs.hmm.2019.03.001.
- [5] M.N. Inallu, P. Kameli, A.G. Varzaneh, I.A. Sarsari, D. Salazar, I. Orue, V.A. Chernenko, Magnetocaloric effect in W-doped Ni-Mn-Sn alloy probed by direct and indirect measurements, *J. Phys. D. Appl. Phys.* 52 (2019) 235001. doi:10.1088/1361-6463/ab0f79.
- [6] J. Liu, N. Scheerbaum, J. Lyubina, O. Gutfleisch, Reversibility of magnetostructural transition and associated magnetocaloric effect in Ni–Mn–In–Co, *Appl. Phys. Lett.* 93 (2008) 102512. doi:10.1063/1.2981210.
- [7] C. Seguí, E. Cesari, P. Lázpita, Magnetic properties of martensite in metamagnetic Ni-Co-Mn-Ga alloys, *J. Phys. D. Appl. Phys.* 49 (2016) 165007. doi:10.1088/0022-3727/49/16/165007.
- [8] N.M. Bruno, C. Yegin, I. Karaman, J.-H. Chen, J.H. Ross, J. Liu, J. Li, J.H. Ross Jr., J. Liu, J. Li, The effect of heat treatments on $Ni_{43}Mn_{42}Co_4Sn_{11}$ meta-magnetic shape

- memory alloys for magnetic refrigeration, *Acta Mater.* 74 (2014) 66–84.
doi:10.1016/j.actamat.2014.03.020.
- [9] P. Lázpita, M. Sasmaz, J.M. Barandiarán, V.A. Chernenko, Effect of Fe doping and magnetic field on martensitic transformation of Mn-Ni(Fe)-Sn metamagnetic shape memory alloys, *Acta Mater.* 155 (2018) 95–103. doi:10.1016/j.actamat.2018.05.052.
- [10] C. Liu, Y. Zhang, Y. Liu, J. Sun, Y. Huang, B. Kang, D. Deng, C. Jing, Z. Li, Y. Zhang, K. Xu, Martensitic transition, inverse magnetocaloric effect and shape memory characteristics in $\text{Mn}_{48-x}\text{Cu}_x\text{Ni}_{42}\text{Sn}_{10}$ Heusler alloys, *Phys. B Condens. Matter.* 508 (2017) 118–123. doi:10.1016/j.physb.2016.12.026.
- [11] D.Y. Cong, L. Huang, V. Hardy, D. Bourgault, X.M. Sun, Z.H. Nie, M.G. Wang, Y. Ren, P. Entel, Y.D. Wang, Low-field-actuated giant magnetocaloric effect and excellent mechanical properties in a NiMn-based multiferroic alloy, *Acta Mater.* 146 (2018) 142–151. doi:10.1016/j.actamat.2017.12.047.
- [12] F.X. Hu, B.G. Shen, J.R. Sun, Magnetic entropy change involving martensitic transition in NiMn-based Heusler alloys, *Chinese Phys. B.* 22 (2013) 0–15.
doi:10.1088/1674-1056/22/3/037505.
- [13] N.A. De Oliveira, Entropy change upon magnetic field and pressure variations, *Appl. Phys. Lett.* 90 (2007) 10–13. doi:10.1063/1.2434154.
- [14] G. Li, J. Wang, Z. Cheng, Q. Ren, C. Fang, S. Dou, Large entropy change accompanying two successive magnetic phase transitions in TbMn_2Si_2 for magnetic refrigeration, *Appl. Phys. Lett.* 106 (2015) 182405. doi:10.1063/1.4919895.
- [15] Z. Li, K. Xu, Y. Zhang, C. Tao, D. Zheng, C. Jing, Two successive magneto-structural transformations and their relation to enhanced magnetocaloric effect for $\text{Ni}_{55.8}\text{Mn}_{18.1}\text{Ga}_{26.1}$ Heusler alloy, *Sci. Rep.* 5 (2015) 1–7. doi:10.1038/srep15143.
- [16] X. Zhang, M. Qian, S. Miao, R. Su, Y. Liu, L. Geng, J. Sun, Enhanced magnetic entropy change and working temperature interval in Ni-Mn-In-Co alloys, *J. Alloys Compd.* 656 (2016) 154–158. doi:10.1016/j.jallcom.2015.09.212.
- [17] L. Mañosa, A. Planes, Materials with Giant Mechanocaloric Effects: Cooling by Strength, *Adv. Mater.* 29 (2017) 1603607. doi:10.1002/adma.201603607.
- [18] L. Mañosa, A. Planes, Mechanocaloric effects in shape memory alloys, *Philos. Trans. R. Soc. A Math. Phys. Eng. Sci.* 374 (2016) 20150310. doi:10.1098/rsta.2015.0310.
- [19] E. Stern-Taulats, T. Castán, L. Mañosa, A. Planes, N.D. Mathur, X. Moya,

- Multicaloric materials and effects, *MRS Bull.* 43 (2018) 295–299.
doi:10.1557/mrs.2018.72.
- [20] A. Czernuszewicz, J. Kaleta, D. Lewandowski, Multicaloric effect: Toward a breakthrough in cooling technology, *Energy Convers. Manag.* 178 (2018) 335–342.
doi:10.1016/j.enconman.2018.10.025.
- [21] I.A. Stepanov, Entropy change in materials under compression and expansion, *Mater. Lett.* 234 (2019) 38–39. doi:10.1016/j.matlet.2018.09.052.
- [22] K.P. Skokov, K.H. Müller, J.D. Moore, J. Liu, A.Y. Karpenkov, M. Krautz, O. Gutfleisch, Influence of thermal hysteresis and field cycling on the magnetocaloric effect in $\text{LaFe}_{11.6}\text{Si}_{1.4}$, *J. Alloys Compd.* 552 (2013) 310–317.
doi:10.1016/j.jallcom.2012.10.008.
- [23] V. V. Khovaylo, K.P. Skokov, O. Gutfleisch, H. Miki, R. Kainuma, T. Kanomata, Reversibility and irreversibility of magnetocaloric effect in a metamagnetic shape memory alloy under cyclic action of a magnetic field, *Appl. Phys. Lett.* 97 (2010) 1–4.
doi:10.1063/1.3476348.
- [24] O. Gutfleisch, T. Gottschall, M. Fries, D. Benke, I. Radulov, K.P. Skokov, H. Wende, M. Gruner, M. Acet, P. Entel, M. Farle, Mastering hysteresis in magnetocaloric materials, *Philos. Trans. R. Soc. A Math. Phys. Eng. Sci.* 374 (2016) 20150308.
doi:10.1098/rsta.2015.0308.
- [25] V. Srivastava, X. Chen, R.D. James, Hysteresis and unusual magnetic properties in the singular Heusler alloy $\text{Ni}_{45}\text{Co}_5\text{Mn}_{40}\text{Sn}_{10}$, *Appl. Phys. Lett.* 97 (2010) 014101.
doi:10.1063/1.3456562.
- [26] J. Liu, T. Gottschall, K.P. Skokov, J.D. Moore, O. Gutfleisch, Giant magnetocaloric effect driven by structural transitions, *Nat. Mater.* 11 (2012) 620–626.
doi:10.1038/nmat3334.
- [27] J.M. Barandiarán, V.A. Chernenko, E. Cesari, D. Salas, J. Gutiérrez, P. Lázpita, Magnetic field and atomic order effect on the martensitic transformation of a metamagnetic alloy, *J. Phys. Condens. Matter.* 25 (2013) 484005.
<http://www.ncbi.nlm.nih.gov/pubmed/24201042>.
- [28] A. Planes, L. Mañosa, M. Acet, Magnetocaloric effect and its relation to shape-memory properties in ferromagnetic Heusler alloys, *J. Phys. Condens. Matter.* 21 (2009) 233201. doi:10.1088/0953-8984/21/23/233201.
- [29] M. Khan, I. Dubenko, S. Stadler, N. Ali, Exchange bias in bulk Mn rich Ni–Mn–Sn

- Heusler alloys, *J. Appl. Phys.* 102 (2007) 113914. doi:10.1063/1.2818016.
- [30] V.O. Golub, V.A. L'vov, I. Aseguinolaza, O. Salyuk, D. Popadiuk, Y. Kharlan, G.N. Kakazei, J.P. Araujo, J.M. Barandiarán, V.A. Chernenko, Antiferromagnetic coupling between martensitic twin variants observed by magnetic resonance in Ni-Mn-Sn-Co films, *Phys. Rev. B.* 95 (2017) 1–8. doi:10.1103/PhysRevB.95.024422.
- [31] V.A. L'vov, E. Cesari, J.I. Pérez-Landazábal, V. Recarte, J. Torrens-Serra, Magnetically driven magnetostructural transformations of shape memory alloys, *J. Phys. D: Appl. Phys.* 49 (2016) 095002. doi:10.1088/0022-3727/49/9/095002.
- [32] V.A. Chernenko, J.M. Barandiarán, J. Rodríguez Fernández, D.P. Rojas, J. Gutiérrez, P. Lázpita, I. Orue, Magnetic and magnetocaloric properties of martensitic Ni₂Mn_{1.4}Sn_{0.6} Heusler alloy, *J. Magn. Magn. Mater.* 324 (2012) 3519–3523. doi:10.1016/j.jmmm.2012.02.080.
- [33] T. Yasuda, T. Kanomata, T. Saito, H. Yosida, H. Nishihara, R. Kainuma, K. Oikawa, K. Ishida, K.-U. Neumann, K.R. a. Ziebeck, Pressure effect on transformation temperatures of ferromagnetic shape memory alloy Ni₅₀Mn₃₆Sn₁₄, *J. Magn. Magn. Mater.* 310 (2007) 2770–2772. doi:10.1016/j.jmmm.2006.10.1043.
- [34] S. Esakki Muthu, N. V. Rama Rao, M. Manivel Raja, S. Arumugam, K. Matsubayasi, Y. Uwatoko, Hydrostatic pressure effect on the martensitic transition, magnetic, and magnetocaloric properties in Ni_{50-x}Mn_{37+x}Sn₁₃ Heusler alloys, *J. Appl. Phys.* 110 (2011) 10–14. doi:10.1063/1.3651375.
- [35] A.K. Nayak, K.G. Suresh, A.K. Nigam, A.A. Coelho, S. Gama, Pressure induced magnetic and magnetocaloric properties in NiCoMnSb Heusler alloy, *J. Appl. Phys.* 106 (2009) 053901. doi:10.1063/1.3208064.
- [36] J. Kaštil, J. Kamarád, O. Isnard, Y. Skourski, M. Míšek, Z. Arnold, Effect of pressure and high magnetic field on phase transitions and magnetic properties of Ni_{1.92}Mn_{1.56}Sn_{0.52} and Ni₂MnSn Heusler compounds, *J. Alloys Compd.* 650 (2015) 248–255. doi:10.1016/j.jallcom.2015.07.284.
- [37] J. Kamarád, F. Albertini, Z. Arnold, S. Fabbri, J. Kaštil, Extraordinary magnetic and structural properties of the off-stoichiometric and the Co-doped Ni₂MnGa Heusler alloys under high pressure, *Acta Mater.* 77 (2014) 60–67. doi:10.1016/j.actamat.2014.06.011.
- [38] J. Kamarád, S. Fabbri, J. Kaštil, M. Míšek, R. Cabassi, F. Cugini, F. Albertini, Z. Arnold, Strong magneto-volume effects and hysteresis reduction in the In-doped

- (NiCo)₂MnGa Heusler alloys, *J. Alloys Compd.* 685 (2016) 142–146.
doi:10.1016/j.jallcom.2016.05.240.
- [39] V. Recarte, J.I. Pérez-Landazábal, V. Sánchez-Alarcos, J.A. Rodríguez-Velamazán, Dependence of the martensitic transformation and magnetic transition on the atomic order in Ni–Mn–In metamagnetic shape memory alloys, *Acta Mater.* 60 (2012) 1937–1945. doi:10.1016/j.actamat.2012.01.020.
- [40] T. Kanomata, K. Shirakawa, T. Kaneko, Effect of hydrostatic pressure on the Curie temperature of the Heusler alloys Ni₂MnZ (Z = Al, Ga, In, Sn and Sb), *J. Magn. Magn. Mater.* 65 (1987) 76–82. doi:10.1016/0304-8853(87)90312-X.
- [41] R.Y. Umetsu, X. Xu, R. Kainuma, NiMn-based metamagnetic shape memory alloys, *Scr. Mater.* 116 (2016) 1–6. doi:10.1016/j.scriptamat.2016.01.006.
- [42] J.M. Barandiarán, V.A. Chernenko, E. Cesari, D. Salas, P. Lázpita, J. Gutiérrez, I. Orue, Magnetic influence on the martensitic transformation entropy in Ni–Mn–In metamagnetic alloy, *Appl. Phys. Lett.* 102 (2013) 071904. doi:10.1063/1.4793412.
- [43] P. Lázpita, M. Sasmaz, E. Cesari, J.M. Barandiarán, J. Gutiérrez, V.A. Chernenko, Martensitic transformation and magnetic field induced effects in Ni₄₂Co₈Mn₃₉Sn₁₁ metamagnetic shape memory alloy, *Acta Mater.* 109 (2016) 170–176. doi:10.1016/j.actamat.2016.02.046.
- [44] V.A. L’vov, A. Kosogor, J.M. Barandiaran, V.A. Chernenko, Theoretical description of magnetocaloric effect in the shape memory alloy exhibiting metamagnetic behavior, *J. Appl. Phys.* 119 (2016) 013902. doi:10.1063/1.4939556.
- [45] D. Comtesse, M.E. Gruner, M. Ogura, V. V Sokolovskiy, V.D. Buchelnikov, A. Grünebohm, R. Arróyave, N. Singh, T. Gottschall, O. Gutfleisch, V.A. Chernenko, F. Albertini, S. Fähler, P. Entel, First-principles calculation of the instability leading to giant inverse magnetocaloric effects, *Phys. Rev. B.* 89 (2014) 184403(1-6). doi:10.1103/PhysRevB.89.184403.
- [46] E. Şaşıoğlu, L.M. Sandratskii, P. Bruno, Pressure dependence of the Curie temperature in Ni₂MnSn Heusler alloy: A first-principles study, *Phys. Rev. B.* 71 (2005) 214412. doi:10.1103/PhysRevB.71.214412.
- [47] I. Rungger, S. Sanvito, Ab initio study of the magnetostructural properties of MnAs, *Phys. Rev. B - Condens. Matter Mater. Phys.* 74 (2006) 1–14. doi:10.1103/PhysRevB.74.024429.
- [48] J. Kamarád, J. Kudrnovský, Z. Arnold, V. Drchal, I. Turek, Pressure effect on

- magnetic moments in ordered Ni₃Mn and disordered Ni_{100-x}Mn_x alloys: Ab initio calculation and experiment, *High Press. Res.* 31 (2011) 116–120.
doi:10.1080/08957959.2010.529808.
- [49] P. Entel, M.E. Gruner, S. Fähler, M. Acet, A. Çahır, R. Arróyave, S. Sahoo, T.C. Duong, A. Talapatra, L. Sandratskii, S. Mankowsky, T. Gottschall, O. Gutfleisch, P. Lázpita, V.A. Chernenko, J.M. Barandiarán, V. V. Sokolovskiy, V.D. Buchelnikov, Probing Structural and Magnetic Instabilities and Hysteresis in Heuslers by Density Functional Theory Calculations, *Phys. Status Solidi Basic Res.* 255 (2018) 1–14.
doi:10.1002/pssb.201700296.
- [50] H. Yan, Y. Zhang, N. Xu, A. Senyshyn, H.G. Brokmeier, C. Esling, X. Zhao, L. Zuo, Crystal structure determination of incommensurate modulated martensite in Ni-Mn-In Heusler alloys, *Acta Mater.* 88 (2015) 375–388. doi:10.1016/j.actamat.2015.01.025.
- [51] T. Kamiyama, T. Shinohara, S. Tomiyoshi, Y. Minonishi, H. Yamamoto, H. Asano, N. Watanabe, Effect of deformation on Pd₂MnSn Heusler alloy studied with transmission electron microscopy, profile analysis of neutron powder diffraction pattern, and magnetization measurement, *J. Appl. Phys.* 68 (1990) 4741–4750.
doi:10.1063/1.346128.
- [52] A.I. Akhiezer, V.G. Bar'yakhtar, S. V. Peletminskii, *Spin Waves*, John Wiley & Sons, North-Holland, 1968. doi:10.1126/science.163.3870.923-a.
- [53] V.A. Chernenko, V.A. L'vov, S.P. Zagorodnyuk, T. Takagi, Ferromagnetism of thermoelastic martensites: Theory and experiment, *Phys. Rev. B.* 67 (2003) 064407.
doi:10.1103/PhysRevB.67.064407.